J Mater Sci (2010) 45:1866–1877
DOI 10.1007/s10853-009-4171-7

Synthesis and characterization of novel THTPBA/PEG-derived polyurethane scaffolds for tissue engineering

Yanling Luo · Changhu Zhang · Feng Xu · Yashao Chen · Lihua Fan · Qingbo Wei

Received: 14 September 2009 / Accepted: 28 December 2009 / Published online: 12 January 2010

Abstract Novel polyurethane (PU) scaffold materials were designed and prepared on the basis of a coupling reaction between tetra-hydroxyl-terminated poly(butadiene-co-acrylonitrile) prepolymer (THTPBA) and poly(ethylene glycol) (PEG) via 1,6-hexamethylene diisocyanate as anchor molecule. The hydrophilicity, degradability, mechanical, and biomedical properties of the THTPBA/PEG PU materials were scrutinized by swelling and goniometry, FTIR and gravimetry methods, tensile stress–strain measurements and hemolysis, platelet activation, dynamic (erythrocyte aggregation) and static coagulation as well as MTT assays. The experimental results indicated that the hydrophilicity and mass loss were enhanced with increased concentrations and molecular weight (MW) of PEG. The degradation may be attributable to the cleavage of urethane or ester bonds in polymer chains. The in vitro blood compatibility and MTT cytotoxicity investigations elicited that the MW of PEG and mass ratios of THTPBA to PEG had important influence on the biomedical properties. The tensile stress–strain investigations showed that the highly cross-linked architecture offered high elastic modulus and mechanical strength. The PU scaffolds with proper component ratios and MW of PEG exhibited improved mechanical properties and biocompatibility as well as low toxicity, and can be employed as potential candidates for blood-contacting applications.

Y. Luo (✉) · C. Zhang · F. Xu (✉) · Y. Chen · L. Fan · Q. Wei
Key Laboratory of Macromolecular Science of Shaanxi Province, School of Chemistry and Materials Science, Shaanxi Normal University, No. 199, South Chang'an Road, 710062 Xi'an, People's Republic of China
e-mail: luoyanl@snnu.edu.cn

F. Xu
e-mail: fengxu@snnu.edu.cn

Introduction

Medical polymers are an emerging cross-discipline dealing with life science, materials science, and polymer chemistry. It is also one of the most important and fastest growing areas in functional polymer sciences and is in the cutting edge of polymer science. Polyurethane (PU) materials have increasingly attracted attention in medical applications in that the majority of the PU macromolecules exhibit favorable biodegradability, biocompatibility, hemocompatibility, and non-toxicity or side effects [1–3]. Their architecture, which contains hard (diisocyanate and chain extender) and soft segments (polyol), provides distinct hard–soft-segmented microphase separation, which imparts elastomeric properties attractive for soft tissue engineering [4]. They therefore have found wide applications in the medical realm of blood-contacting biomaterials, such as vascular grafts, catheters, general-purpose tubing, and artificial hearts to promote regeneration of cells and tissues, such as long-term implantable medical devices and artificial organs [5, 6].

Despite the development of a large number of the PU polymers as tissue engineering applications, the majority of them are composed of linear aliphatic polyesters with high MW and their copolymers, thus they are often utilized in hard tissue engineering because of their high glass transition temperature and high modulus [7]. On the other hand, the majority of medical blood-contacting PUs containing polyether-based polyol soft segments bears rapid degradation rate, limiting broader clinical

applications. The choice of scaffolds is one of the focal points in tissue engineering research. The elastic or flexible stents can be used for soft tissue engineering as their mechanical properties can readily be controlled or tailored in accordance with the developing requirements for tissue engineering. Effort to develop such soft tissue engineering materials as cardiac, vascular and skeletal muscle, and adipose tissue even cartilage tissue as well as ureteral stents is one of the most challenging and therefore the most difficult subjects in the realm of tissue engineering. Those three-dimensional scaffold materials that match the mechanical properties are the preferred soft tissue engineering materials. This type of scaffold materials can not only be used as a structural support, but also can promote cell adhesion, growth, and angiogenesis during the in vitro cell culture and in vivo tissue regeneration process.

It is known that the performances of cells and tissues on the materials are affected by the chemical structure, electric charge, hydrophilicity and hydrophobicity, surface roughness, microheterogeneity, and flexibility of the materials [8]. Considering the amphiphilicity, definite surface activity, good biocompatibility, non-toxicity, low immunogenicity of polyethylene glycol (PEG) [9, 10], we can hypothesize that PEG is used as a main constituent, while a hydrophobic reactive prepolymer with multifunctional groups terminated is inserted in the PEG-based PU backbone so as to constitute a mechanical support with a soft-segmented phase separation. This combination is anticipated to influence or alter surface properties, even hemocompatibility of the PEG-derived PU biomaterials. Yang et al. has reported HTPB-based PU films to improve the blood compatibility and wettability of the material [10].

Based on the above consideration, the objective of this work is to design and prepare a novel PU scaffold with improved mechanical and biomedical properties, which is expected to potentially be employed in tissue engineering as temporary mechanical scaffolds. The focus is on the assessment of mechanical and biomedical properties of the highly branched or crosslinked PU materials, and the in vitro degradation behavior is also portrayed to provide insight into the degradation mechanism of the polymers. As far as we know, the present research is the first attempt to modulate or tailor mechanical and biomedical properties for promising bio-applications in the realm of tissue engineering. Compared with traditional linear PU analogues, the as-prepared PUs exhibit interesting and versatile performances, and is expected to have advantages over traditional PU formulations in biocompatibility (thromboresistance, etc.), cytotoxicity, degradation, and mechanical properties.

Experimental details

Materials

Carboxyl-terminated poly(butadiene-co-acrylonitrile) oligomer (CTBN) was purchased from the Zibo Qilong Chem. Corp. (Shandong, China), with MW of 2,500 and carboxyl groups of 5.878×10^{-4} mol (g^{-1} CTBN). Triethanolamine, analytical grade (TEA, A.G.), was provided by the Hongyan Reagent Factory (Tianjin, China). PEG, biologic grade (B.G.), with MW of 1,000, 4,000, 10,000, and 20,000, was supplied by the National Pharmaceutical Ind. Corp. (Tianjin, China). The 1,6-hexamethylene diisocyanate (HDI, A.G.) was obtained from the Shanghai Sigma–Aldrich Trading Corp. Ltd. Human embryonic kidney (HEK) cell was obtained from the Lanzhou Minhai Corp., China. The dimethyl sulfoxide (DMSO) and 3-(4,5-dimethylthiazol-2-yl)-2,5-diphenyltetrazolium bromide (MTT) were provided by the Paini Chemical Reagent Factory (Henan, China). Trypsin (0.25 wt% in a phosphate buffer solution, PBS) was obtained from the Beijing Solarbio Sci. Technol. Corp., Ltd. All other chemicals and solvents were of analytical grade, and used as received.

Synthesizing procedures

THTPBA/PEG PU scaffolds were prepared according to the following procedure. CTBN was first hydroxyl-functionalized by an esterification route, as illustrated in Scheme 1. Typically, 14.6 g CTBN and 35 mL excess TEA were added into a three-necked flask equipped with a magnetic stirrer. After dissolved and fully mixed under stirring, 4 mL H_2SO_4–water mixture solution (volume ratio of 5:1) was introduced into the solution. The reaction mixture was heated up to 110 °C, and the esterification reaction proceeded for 24 h. After that, the viscous product was cooled till room temperature. Subsequently, it was immersed in distilled water several times until pH about 7.0 to remove the catalyst and unreacted TEA, accompanied by mechanical stirring. After dried at 70 °C in a vacuum oven for 5 days, a hydroxyl-functionalized CTBN modified by the TEA, viz., tetra-hydroxyl-terminated poly(butadiene-co-acrylonitrile) prepolymer (THTPBA), was acquired.

The obtained THTPBA was completely dissolved into a 40 mL cuvette of 10 mL toluene (note: remove water with calcium hydride beforehand) at mass ratios of THTPBA to PEG 1:0, 3:7, 5:5, 7:3, and 0:1. Subsequently, a given molar coefficient r of HDI ($r = 1.1$, r is defined as a ratio of –NCO moles to the total –OH moles of the THTPBA and PEG, i.e., $r = (\text{–NCO/–OH})_{\text{mol}}$) was added, and simultaneously accompanied by 2–3 drops of dibutyltin

Scheme 1 Synthetic route sketch of representative THTPBA/PEG PU scaffolds

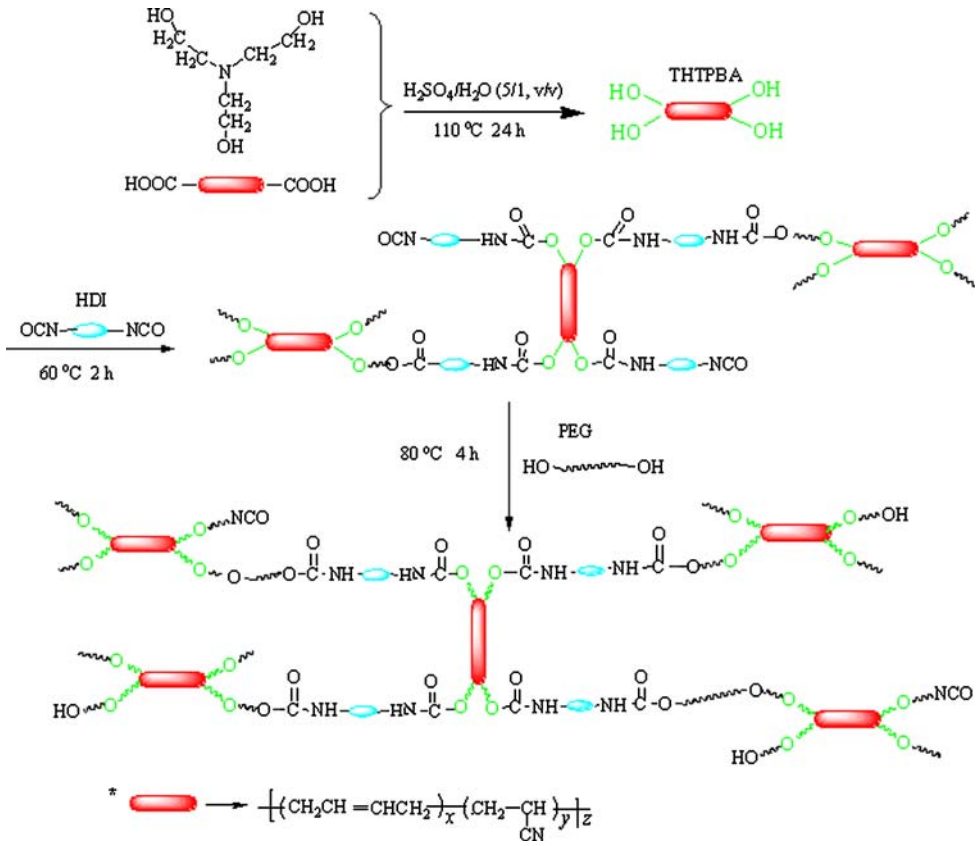

dilaurate (DBTDL). The mixture solution was bubbled with N_2 for 30 min to remove the dissolved oxygen, and then the cuvette was sealed and immersed in a 60 °C water bath for 120 min under stirring. Afterwards, a 5 mL toluene solution of PEG was plunged into the above solution, accompanied by another one drop of DBTDL. The reaction proceeded at 80 °C for another 4 h, and the viscous products were transferred into a glass mold of 6.0 cm × 5.0 cm × 0.25 cm. After volatilized and solidified at 60 °C for 24 h in a drier, a sheet-like PU copolymer was obtained.

FTIR

A Fourier transformation infrared spectrometer with the attenuated total reflection (FTIR-ATR, Equinx55, Bruker, Germany) was utilized to inspect the main chemical structure changes of THTPBA/PEG-derived PU samples before and after hydrolytic degradation.

Hydrophilicity

Swelling measurement

The equilibrium swelling ratios (R_e) were determined gravimetrically by allowing an accurate amount of PU sheet samples to reach an equilibrium state in water at 25 °C. After fully hydrating, the samples were taken out and the excess water was gently removed by filter paper. The R_e values were calculated as the following equation [11]:

$$R_e = [(W_e - W_d)/W_d]100\% \quad (1)$$

where W_e and W_d stand for the mass of samples in an equilibrium state and dried samples, respectively.

Goniometry

Contact angle measurements were made on the surface of THTPBA/PEG-based PU samples to gauge the effect of different feed ratios and MW of PEG on surface hydrophilicity, a vital parameter influencing blood–material interactions. Contact angles were measured using a sessile drop method on a video-based contact angle measuring device (OCA20, Dataphysics, Germany). Briefly, samples were laid on the platform, and then one drop (2 μL) of water was layered mechanically with a syringe onto the surface of the samples. The image of the droplet was analyzed using the in-built software. The contact angle was measured as an average angle between the sample surface and the tangent drawn to the surface of the droplet at the interface at the right and left extremities of the droplet. All

reported contact angle data are presented as mean values ± standard deviations of 5 measurements on each specimen.

Mass loss measurements

The mass loss of degraded products was measured by gravimetry reported elsewhere [11, 12]. The dried samples (W_0) were immersed in a 25 mL PBS of pH 7.4 at 37 °C for 10–120 days. The degraded samples were then immersed in distilled water again and rinsed with distilled water several times to discard salt. After the samples were dried at 60 °C for 24 h in an oven, and weighed (W_d). Mass loss (%) of the samples was calculated according to the following formula:

$$\text{Mass loss} = [(W_0 - W_d)/W_0]100\% \quad (2)$$

Mechanical properties

A floor-standing electromechanical universal testing machine (CMT2000, MTS System (China) Co., Ltd., Shenzhen) was employed to measure the tensile mechanical properties of the PU samples according to ASTM D 638M-84. The tests were performed at a crosshead speed of 10 mm min^{-1} on dumbbell specimens about 0.4 mm thickness at room temperature. All mechanical analyses were conducted at least in quadruplicate for each specimen to produce an average value.

Blood compatibility analysis

Blood and plasma

Blood and plasma treatment were conducted in terms of the literature [13]. Blood was drawn from healthy donors into an evacuated siliconized glass tubes containing 3.2% sodium citrate or heparinized sodium (the volume ratio of blood to anticoagulant 9:1). Platelet poor plasma (PPP) was isolated by centrifuging at 3000 rpm for 15 min at room temperature and used immediately. Platelet rich plasma (PRP) was isolated by centrifuging the citrated blood or heparin sodium at 800 rpm for 15 min followed by pipetting out the supernatant plasma containing the platelets. The platelet count in the PRP was adjusted to 180×10^9 L^{-1} with plasma.

In vitro hemocompatibility tests

The in vitro blood compatibility was investigated by hemolysis assay, clotting assays, and blood platelet adhesion tests.

Hemolysis assay Human blood was used to test the hemolysis effect of the as-prepared samples. Briefly, sheet samples were cut into small pieces, and equilibrated in a 0.9% normal physiologic saline at 25 °C for 30 min and washed 3 times. Then, 4 mL acid citrate dextrose (ACD) blood was added to a 6 mL physiologic saline, and a diluted blood solution was attained. After a predetermined period of time, another 10 mL physiologic saline and 0.2 mL diluted blood solution were added into their respective sample tubes. An identical set of samples was kept at 37 °C for 60 min. In comparison, positive and negative controls were produced by adding 0.2 mL of diluted human blood to 10 mL of distilled water and 10 mL physiologic saline water, respectively. After marinating, all the sample tubes were centrifuged at 1000 rpm for 15 min. The mixtures were then aspirated, and the absorbance of the clear supernatant was measured by a TU-1901 UV–vis spectrophotometer (Beijing Puxi General Instrument Co. Ltd, China) at 545 nm. The hemolysis ratio (HR) was presented as the equation [14]:

$$\text{HR}\% = \left[\frac{\text{OD}_{\text{of test sample}} - \text{OD}(-)_{\text{control}}}{\text{OD}(+)_{\text{conrtrol}} - \text{OD}(-)_{\text{control}}}\right] \times 100\% \quad (3)$$

where OD denotes optical density.

Dynamic clotting time measurement For clotting time measurement, 20 μL of human blood anticoagulated by ACD was first dripped on the sample surface in an open atmosphere at room temperature (25 °C). Clotting was initiated by the addition of 4 μL of 0.2 M $CaCl_2$ solution. After 5, 10, 20, 30, 40, and 50 min, each sample was transferred into a big cuvette containing 40 mL of distilled water. Then the optical density of the supernatant was measured at 540 nm using the above UV–vis spectrophotometer. For each coating, an average optical density was obtained for three measurements.

Prothrombin time and activated partial thromboplastin time For the prothrombin time (PT) determination, the extrinsic and common coagulation was activated by incubating plasma with a STA-Neoplastine CL® reagent (Diagnostica Stago, France) and the clotting time was then measured. The activated partial thromboplastin time (APTT) is a simple and highly reliable measurement of the capacity of blood to coagulate through the intrinsic coagulation mechanism with a STA-C.K. Prest® reagent (Diagnostica Stago, France) and of the effect of the biomaterials on possible delay of the process. The PU samples were incubated in 600 μL PPP at 37 °C for 5 min, and then cuvette-strips of the samples were placed in a completely automatic coagulometer (Sysmex CA-1500, Sysmex, Japan). Shortly, the 100 μL PT or 50 μL APTT reagent containing 0.025 M $CaCl_2$ was automatically added, and the time for the onset of clot formation was simultaneously

detected ($n = 6$). Control experiment was done in the same way as the operation without PU samples.

Plasma recalcification time For plasma recalcification time (PRT) measurements, a 0.1 mL 0.025 M $CaCl_2$ solution was introduced into a series of the cuvette-strips holding about 0.025 g PU samples, and then 200 μL human plasma from which the Ca^{2+} was removed (Xi'an Central Blood Bank, China) was added at 37 °C. After the recalcified plasma was immediately stirred with a small stainless steel hook, The PRT was recorded until the silky fibrin appeared. Each experiment was repeated 3 times.

Static platelet adhesion observations

Activation of adhered platelets was assessed through material-induced changes in the morphologies of adhered platelets on representative PU samples, visualized using SEM (Quanta 200, Philips-FEI, The Netherlands) with an operating voltage of 20 kV. Before measurement, the PU samples were immersed in alcohol solution for 2 min, and then washed 3 times by 15 mL distilled water, and eventually immersed in physiologic saline for 24 h. After predetermined manipulation, the samples were put into the cuvette, and aliquots (1 mL) of PRP (platelet suspensions containing 2.5–4.0 $\times$ 10^8 platelets mL^{-1}) were added into each tube and incubated at 37 °C for 1 and 12 h, respectively. After incubation, the PRP was taken out from the tubes. A PBS (pH 7.4) was added to the wells and gently rinsed 2–3 times to get rid of the platelets adsorbed loosely on the sample surface. The samples were then soaked in 2.5 wt% glutaraldehyde at room temperature for 12 h to fix the adhered platelets, followed by dehydration in 50, 75, 95, and 100% (v/v) ethanol/water for 10–15 min. After that, the residual alcohol on the samples was cleaned off in 50, 75, 95, and 100% (v/v) isoamyl acetate/ethanol solutions for 10–15 min. After CO_2 critical-point drying (Hitachi HCP-2 Critical Point Dryer), the samples were coated with gold films over 90 s in sputter coater and the distribution and morphology of the platelets were observed at 20 kV accelerating voltage.

Cytotoxicity assay

Before assay, cell culture was conducted first. Typically, the HEK cell was maintained or seeded in RPMI 1640 medium (Invitrogen Corp, USA) at 37 °C in a humidified 5% CO_2 atmosphere, supplemented with 10% (v/v) fetal bovine serum, 20 μg mL^{-1} penicillin–streptomycin and 2.0 mM L-glutamine (all Gibco, Paisley, Scotland, UK). Cytotoxicity assay was carried out in the presence of the highly crosslinked PU polymers by a 96-wells universal microplate reader (EL_x800UV, Bio-Tek, USA) using the MTT test [1]. Cells (2×10^4 cells $well^{-1}$) were first seeded in 96-well plates and incubated with 0.025 g PU specimens, at 37 °C in 5% CO_2 for 1–5 days, 20 μL $well^{-1}$ of 5 mg mL^{-1} MTT solution was added into each well and the plates were incubated for another 4 h. The supernatant was removed carefully, and formazan crystals were solubilized in 200 μL of DMSO. The OD was monitored at 490 nm. Cells incubated without PU polymers were used as a control. The cell viability of the HEK cell on the surface of the PU samples was expressed using the following equation [15]:

$$\text{Cell relative viability } \% = (\text{OD}_{\text{samples}}/\text{OD}_{\text{control}}) \times 100\% \quad (4)$$

All experiments were performed at least in triplicate. The Student's t test was used to determine the significance of any pairs of observed differences. Differences were considered statistically significant $p < 0.05$. All quantitative results are reported as mean values ± standard deviation.

Results and discussion

FT-IR analysis

As an effort to develop the novel polymers, triethanolamine is introduced onto a hydrophobic CTBN via an esterification reaction, thus giving rise to a tetra-hydroxyl-terminated prepolymer, THTPBA. The improved THTPBA is incorporated with hydrophilic PEG via a coupling reaction by means of an anchor molecule HDI, resulting in a highly branched structure, as shown in Scheme 1. FT-IR is used to examine structural information of the as-prepared PU scaffold materials, as depicted in Fig. 1. A distinct absorption peak at 2275–2250 cm^{-1} reflects the stretch vibration of –NCO groups (Fig. 1a). THTPBA samples displays a broad characteristic absorption of –OH groups at 3367 cm^{-1}, and characteristic vibration peaks at 2933 and 2852 cm^{-1} assigned to $–CH_2$ stretch, at 1746–1691 cm^{-1} attributable to –C=O and at 1624 and 914 cm^{-1} (weak peak) ascribed to –C=C– bonds. The peaks at 1405 and 1022 cm^{-1} are related to C–O stretch vibration of an ester bond and $–CH_2$–OH groups originating from the CTBN skeleton itself and the TEA introduced, respectively. The characteristic absorption of –NCO groups, however, becomes weak or disappears after reaction (Fig. 1c, d), while the peaks at 1543, 1264, and 805 cm^{-1} represent characteristic absorptions of carbamate bonds [16], indicating the formation of a THTPBA/PEG-derived PU scaffold. Although the peak at 3425 cm^{-1} in curve c is somewhat weaker than the THTPBA, this vibration band can still testify the existence of the –OH and the

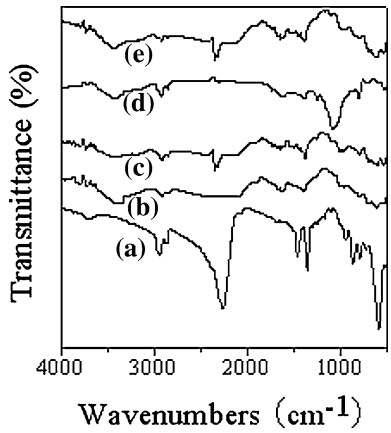

Fig. 1 FT-IR spectra of *a* HDI, *b* THTPBA, *c*, *d* an original THTPBA/PEG PU sample, and *e* degradation residues after 120 days in PBS at pH 7.4 and 37 °C

newly-formed –NH– functional groups on the surface of the PU scaffolds. The existence of characteristic peaks of the THTPBA and PEG (1110 and 841 cm^{-1} attributed to stretching vibration modes of –C–O–C– and $–CH_2CH_2O–$, respectively) [17] and weakening or disappearance of –NCO groups in the resulting products further corroborates the formation of a PU scaffold.

Hydrophilicity

Hydrophilicity of biomaterials is very significant for biocompatibility. Hence equilibrium swelling ratios and surface contact angles of the as-prepared PU samples have been detected to evaluate hydrophilicity or biocompatibility of biomaterials, as depicted in Fig. 2. Unless otherwise specified, the MW of PEG is 10,000, and the mass ratio of THTPBA to PEG10000 is 3:7. It is clear from Fig. 2a that the prepared THTPBA/PEG PU samples display much lower water sorption capacity than a pure PEG PU system. The degradation effect can be neglected owing to their tiny loss during swelling course of 10 days (Fig. 3). The equilibrium swelling ratios are gradually reduced with increasing mass ratios of THTPBA to PEG and decreasing MW of PEG, which is probably attributed to hydrophobicity of THTPBA chains and the highly branched or crosslinked structure of the PU samples. In fact, the pure PEG system produces a multiple increase in swelling capacity in comparison with the dry modality while the R_e of pure THTPBA samples reaches no more than 25%. With increasing MW of PEG, hydrophilic ether groups in PEG chains seem to be more dominant than the end methoxy groups, and hence surface hydrophilicity of PEG soft segments is improved, leading to a higher swelling ratio [18]. Another crucial factor judging the relative hydrophilicity and hydrophobicity of the synthesised PU scaffolds in contact with water is the surface contact angle [19]. Numerous studies have shown that surface structure and properties such as surface roughness, surface hydrophilicity has a decisive role in increasing the blood compatibility [20]. The contact angles are augmented with the increase of the feed ratio of THTPBA to PEG (Fig. 2b), as expected, indicating that the hydrophilicity becomes weak [21, 22], which originates from the insertion of a hydrophobic THTPBA component in the PU structure. These conclusions are well in agreement with each other. The contact angles are slightly increased with increased MW of PEG except that the sample prepared with PEG20000 shows a decreased value. Therefore, the surface properties of the as-prepared biomaterials can also be manipulated and tailored by altering the composition proportion or incorporating different MW of PEG.

Hydrolytic degradation studies

The degradation process is accompanied by mass loss of the PU scaffolds, as shown in Fig. 3. The mass loss is

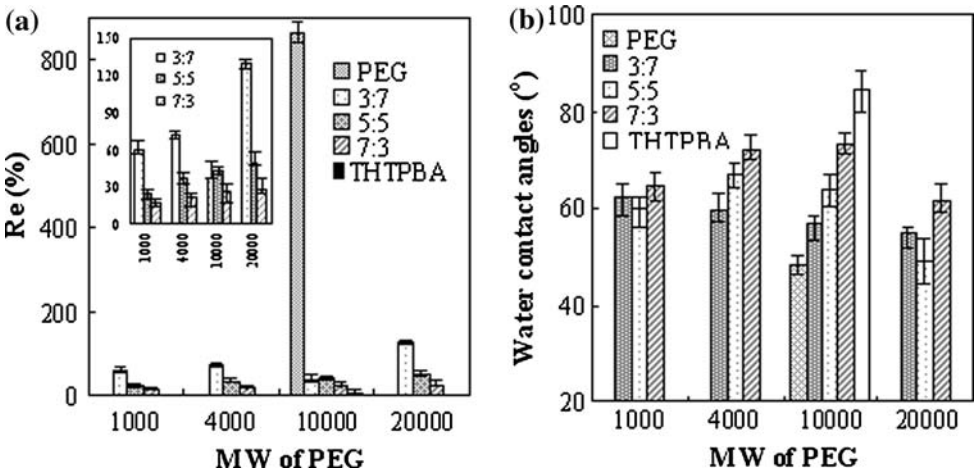

Fig. 2 Dependence of **a** swelling (the *insert* clearly shows R_e variations) and **b** contact angles of the as-prepared PU scaffolds on mass ratios of THTPBA to PEG, and MW of PEG

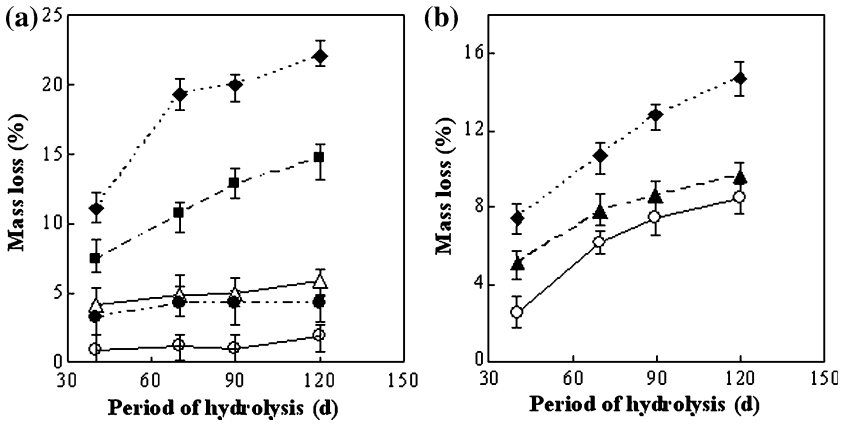

Fig. 3 Mass loss of the THTPBA/PEG-based PU samples after incubation in PBS at pH 7.4 and 37 °C. **a** Effect of the charge ratio of THTPBA to PEG: *filled diamond* blank PEG; *filled square* 3:7; *open triangle* 5:5; *filled circle* 7:3; *open circle* THTPBA. **b** Effect of MW of soft segment PEG: *filled triangle* 1,000; *open circle* 4,000; *filled diamond* 10,000

considerably increased with an increase in degradation time at component ratios of THTPBA to PEG below 5:5, while more than the ratio, a plateau is observed. The degradation is reduced with decreasing PEG contents. Particularly for THTPBA-based samples, the curve of mass loss is close to a straight line parallel to the *x*-axis, implying better degradation stability. It is interesting to correlate the degradation with the MW of PEG, as demonstrated in Fig. 3b. The mass loss of the copolymers is distinctly increased with increasing the MW of PEG during the whole hydrolytic degradation. The lower mass loss of the PU materials with low MW of PEG is attributed to more coupling dots in the highly crosslinked architecture. To sum up, the mass loss clearly indicates that THTPBA/PEG-based PU materials show certain degradation, and the hydrolytic degradation can be controlled by the regulation of polymer compositions, designation of MW of PEG to adapt to specific bio-applications. FT-IR was employed to inspect the structural alterations of different polymeric segments after degradation for 120 days (Fig. 1e). The hydrolytic degradation may be involved in the change in several functional groups, such as –OH, –COO–, –NCO, and –C=O of the carbamate linkage. They appear at ca. 3220–3450, 1694–1735, 2354, and 1639 cm^{-1}, respectively, regardless of original un-decomposed or degraded PU samples. Although a slight mass loss takes place, tiny differences can be perceived. After degradation for 120 days, a broadened absorption band at about 1735–1639 cm^{-1} for the degradation residues, regardless of the feed ratios, is detected and the height ratio of the peaks 1735, 1694, and 1639 cm^{-1} distinctly declines. The absorption change of isocyanate groups can not be distinguished because of the interference of cyanogen groups. On the other hand, we notice that a shoulder peak at ca. 3200–3280 cm^{-1} becomes somewhat evident with degradation proceeding, which may reflect a slight increase in the number of hydrogen bond associated –OH groups originating from the hydrolytic degradation to form a little amount of PEG or THTPBA, even degradation products, TEA and CTBN. Weak changes in width and height of the peak at 3450 cm^{-1} indicate that a very small number of –NH– groups in PU samples may be transferred into –NCO groups, including free hydroxyl groups. The alteration in intensity of $–CH_2CH–$ bands also provides additional information for the hydrolytic degradation of the as-synthesized PU samples. These results prove that the degradation of the urethane or ester linkage takes place.

Mechanical properties

To appraise the role of the highly branched or crosslinked architecture of the new PUs incorporated with different contents of THTPBA on the mechanical properties, the tensile tests were carried out for this series of PU samples. The stress–strain results are summarized and presented in Table 1. It is well-known that the network structures are favorable for reinforcing mechanical strength [23]. Since multiple active-OH groups on the surface of modified THTPBA can couple with –NCO groups, THTPBA/PEG PU networks with a highly crosslinked architecture occur based on chemical interactions between THTPBA and PEG. Higher contents of THTPBA result in more networks in the new PU scaffolds. Therefore, ultimate tensile strength and Young's modulus are markedly increased with increasing percentage content of THTPBA in the PU scaffolds, while elongation at break is decreased, as expected. The enhanced mechanical properties which results from the highly crosslinked architecture may, therefore, be expected to be advantageous for use in situations where increased mechanical performance is required, such as ureteral stents or anklebone, as these PU materials would be less likely to undergo constriction or kinking [24]. The MW of PEG exerts no substantial effect on the tensile properties at break. These samples possess a similar tensile strength and elongation at break, while their elastic modulus is lowered as the MW of PEG is increased below 4,000. This is thought to be due to the large MW of PEG, which provides the soft segments with a decreased number

Table 1 Tensile properties of various highly crosslinked polyurethane samples at ambient temperature

	Tensile strength (MPa)	Elongation at break (%)	Young's modulus (MPa)
Mass ratio of THTPBA to PEG4000			
3:7	18.74 ± 0.12	82.58 ± 0.07	9.479 ± 2.56
5:5	28.62 ± 0.11	30.18 ± 1.12	40.26 ± 3.66
7:3	43.47 ± 0.09	20.12 ± 0.86	91.71 ± 4.11
MW of PEG (mass ratio of THTPBA to PEG 7:3)			
1,000	41.15 ± 0.14	14.65 ± 0.02	127.43 ± 5.23
4,000	43.47 ± 0.09	20.12 ± 0.86	91.71 ± 4.11
20,000	40.60 ± 1.24	10.39 ± 0.35	177.30 ± 5.23

of urethane linkages and increased chain flexibility. Surprisingly, the PU sample with MW of PEG 20,000 has a high deformation-resistance ability, whose Young's modulus reaches up to ca. 177.30 MPa, presumably owing to increased crystallinity [18, 25].

Biomedical properties

The hemolysis ratio and dynamic clotting time

The hemolysis studies reveal hemolytic activity in polymers, and the percentages of hemolysis of heparinized ACD blood for the present polymers are listed in Table 2. It is obviously observed that the hemolysis ratio is less than 2% in all the cases, which comes well within acceptable limit of 5% [1, 26], implying excellent biocompatibility. The hemolysis ratio is enhanced with increasing the component ratios of THTPBA to PEG, and PU materials with high PEG MW have better biocompatibility. A possible explanation is that PEG has better hydrophilicity than THTPBA and surface free energy close to vascular endangium, which is closely correlated to the adsorption and degeneration of blood and so on [27].

The adhesion of globulin and fibrinogen on implants is an important step in the process of thrombus formation, which occurs when activated platelets secrete substances that enzymatically activate otherwise inactive clotting factors. With the help of the dynamic clotting time measurement, the extent that various materials influence thrombus factor can be acquired [28]. The absorbance is directly proportional to the relative volume of non-coagulated red blood cells. It can be noticed from Fig. 4 that for all PU scaffolds the optical density declines significantly with time, the clotting time is shortened and the level of clotting is aggravated. Hereby, the dissociative red cells are dramatically reduced. Figure 4a also shows that the examined PEG specimens have a higher absorbance than THTPBA, while the specimen with THTPBA to PEG ratio 3:7 appears to possess the highest absorbance and a smoother variation of the optical densities than any other systems, and the dissociative red cells are decline slightly, meaning a longer clotting time or a good anticoagulation character [29]. From Fig. 4b, it can be observed that the optical densities are elevated with increasing the MW of PEG except an abnormally low value for PEG20000 specimen because of poor solubility and uniformity. In the case of the PEG10000 PU specimen, a smooth variation of the optical densities and the highest absorbance give rise to, while for other specimens the optical densities abruptly trail off, and a smooth change occurs after about 20 min.

In vitro (anti)-coagulation studies

A change in plasma coagulation properties upon incubation with the biomaterials is an indication of its interaction with blood components which might result in thrombosis [13]. To assess the in vitro (anti)-coagulation of the newly developed PU materials, three kinds of in vitro assays of static clotting time, PT, APTT, and PRT, were performed in PPP or blood plasma, as summarized in Figs. 5 and 6.

For the PT determination, it is noticed that the coagulation time of these samples in PPP is slightly longer than the control, indicating improved blood compatibility. This may be because one of the exogenetic coagulation factors,

Table 2 Hemolysis ratio of the highly crosslinked polyurethane samples with various compositions and PEG MW

Mass ratio of THTPBA to PEG	Hemolysis ratio (%)	MW of PEG	Hemolysis ratio (%)
Pure PEG	0.6229 ± 0.0324	1,000	0.8735 ± 0.0673
3:7	0.7472 ± 0.0532	4,000	1.1032 ± 0.0985
5:5	0.8348 ± 0.0549	10,000	0.7472 ± 0.0532
7:3	0.8579 ± 0.0705	20,000	0.7618 ± 0.0674
Pure THTPBA	1.6845 ± 0.1528		

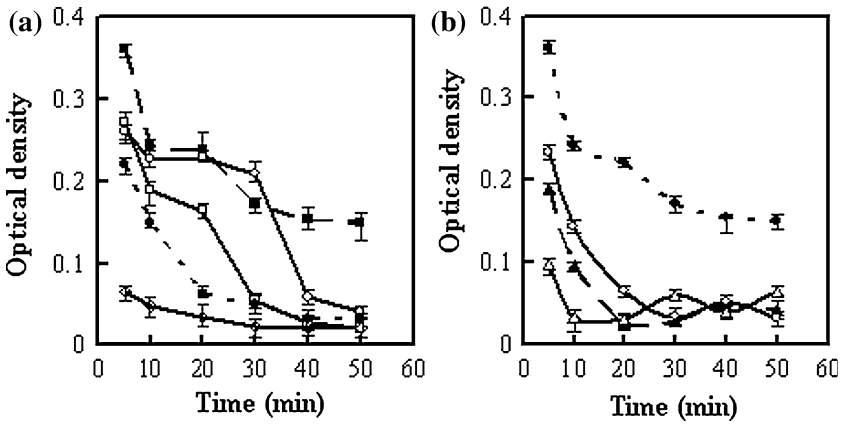

Fig. 4 Dependence of optical density on clotting time for the resulting THTPBA/PEG PU scaffolds with **a** different feed ratios of THTPBA to PEG (*open square* pure PEG; *filled square* 3:7; *open circle* 5:5; *filled circle* 7:3; *open diamond* pure THTPBA) and **b** various MW of PEG (*filled triangle* 1,000; *open circle* 4,000; *filled circle* 10,000; *open triangle* 20,000 in a dynamic clotting test

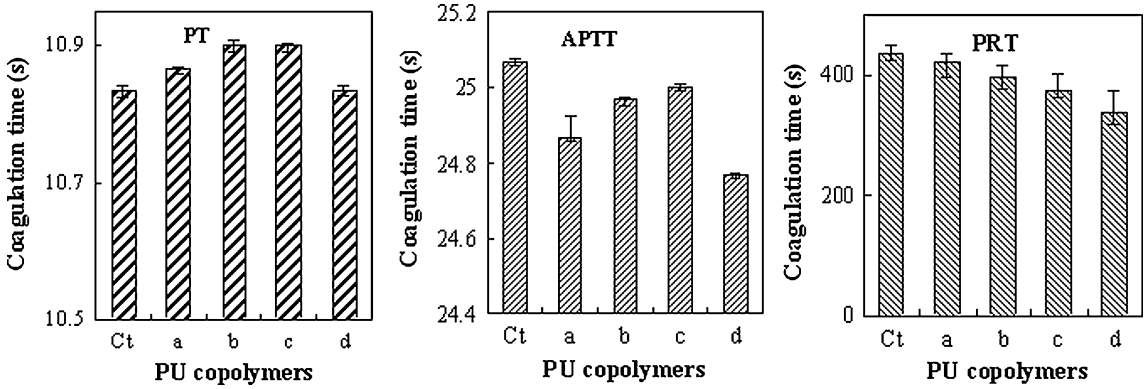

Fig. 5 Effect of various mass ratios of THTPBA to PEG (*Ct* control sample, *a* pure PEG, *b* 3:7, *c* 7:3, *d* pure THTPBA) for PU samples on coagulation time, PRT, PT, and APTT. A final product of about 0.025 g in the cuvette is used in PPP at 37 °C, while PRT is achieved in the blood plasma

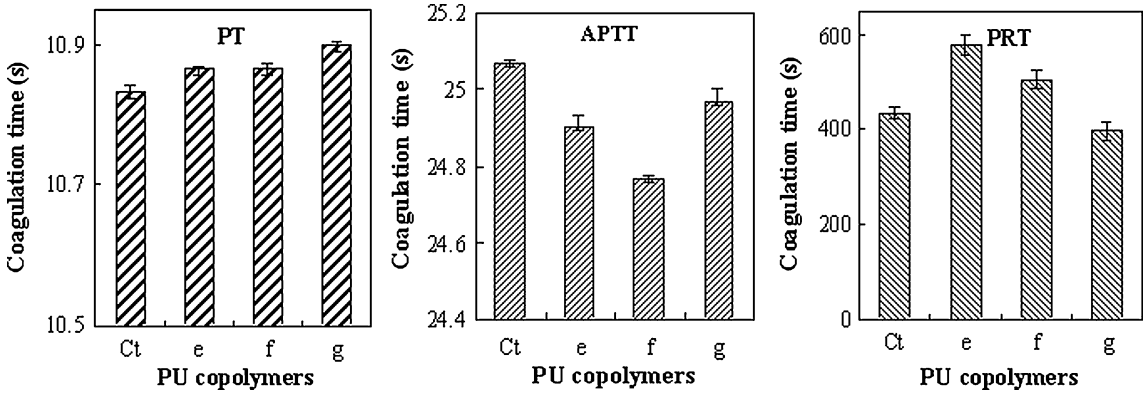

Fig. 6 Effect of different MW of PEG (*Ct* control sample, *e* 1,000, *f* 4,000, *g* 10,000) of identical THTPBA/PEG feed ratio (3:7) for PU samples on coagulation time, PRT, PT, and APTT. A final product of about 0.025 g in the cuvette is used in PPP at 37 °C, while PRT is achieved in the blood plasma

such as thrombogen (II), V, VII, X, and fibrinogen, is likely little reduced or killed [30]. Overall, there is no statistically significant difference in PT, and the as-prepared PU polymers do not significantly alter the clotting time, rate of clot formation or the clot strength, and therefore do not affect the extrinsic coagulation pathway. The APTT time of all the samples is shorter than the control, indicating that the examined PU scaffold samples may activate the

coagulation process. The PT or APTT is prolonged with increasing the THTPBA, and the proper combination of THTPBA with PEG may produce the optimal PT or APTT. Consequently activation of the blood coagulation system is suppressed by the THTPBA/PEG systems, and the extent of suppression is related to the component ratios (Fig. 5). Hence, the blood compatibility of the final samples is improved. Nevertheless, an identical slight difference in APTT (24.70–25.07 s) implies that the PU samples do not interfere with the coagulation time under these nearly physiological conditions, and the observed change might be ascribed to the interference with the activation by the thromboplastin reagent [13]. Therefore, APTT alone cannot always be taken as an indication of biomaterial induced anticoagulant activity. It is to be noted that APTT is only a standardized modification of PRT performed with the use of a coagulation activator. PRT reflects more closely the in vivo situation than activated assays as the activators might mask the polymer effect on coagulation [13].

The PRT is a measurement of the intrinsic coagulation cascade activation defined by the time required for fibrin clot formation once calcium has been introduced into sodium citrate anticoagulated plasma. The PRT of our polymers is significantly different, depending on the feed ratio and MW of PEG. The higher the feed ratio is, the shorter the coagulation time is, as denoted in Fig. 5. This is probably due to an alternatively predominating hydrophilicity or hydrophobility effect originating from PEG and THTPBA, respectively. Meanwhile, the PRT is obviously shortened with increasing the MW of PEG, viz., the samples with low MW of PEG have prolonged PRT, and thus better blood compatibility than the blank sample (Fig. 6). We speculate that this may be attributable to more compact networks from shorter PEG chains, which may prevent protein adsorption and thus improve the blood compatibility. These suggest that the PU samples can impair the activation of the endogenetic cascade in plasma, and the PRT results can be used as an indicator of blood–biomaterial interactions. Since PRT experiments are more close to in vivo conditions, we believe our polymers may induce improved blood compatibility to some extent by suppressing the activation of coagulation factors.

Morphologies of the static adhered platelets in vitro

Since platelet adhesion on the surface of biomaterials is significantly related to the process of protein adsorption and thrombus, the antithrombotic effects of the prepared THTPBA/PEG-based PU samples have been examined by assaying platelet adhesion and activation. Generally speaking, when the materials contact with blood, proteins are first adsorbed instantaneously onto the surfaces of the materials and deformed, and then platelets are adsorbed, activated, and aggregated [31]. Platelets play a major role in the thrombus formation. Therefore, a study on platelets adhesion to evaluate the blood compatibility of biomaterials is important. Figure 7 shows the morphologies of platelets adhered onto the surfaces of various PU samples. Although PEG is well-known for its hydrophilicity, large excluded volume, and unique coordination with surrounding water molecules in an aqueous medium [31], it does not exhibit an extraordinary ability to resist protein adsorption. It is obvious that the platelets adhered onto PEG or THTPBA PU scaffolds (Fig. 7a, d), are spread and have

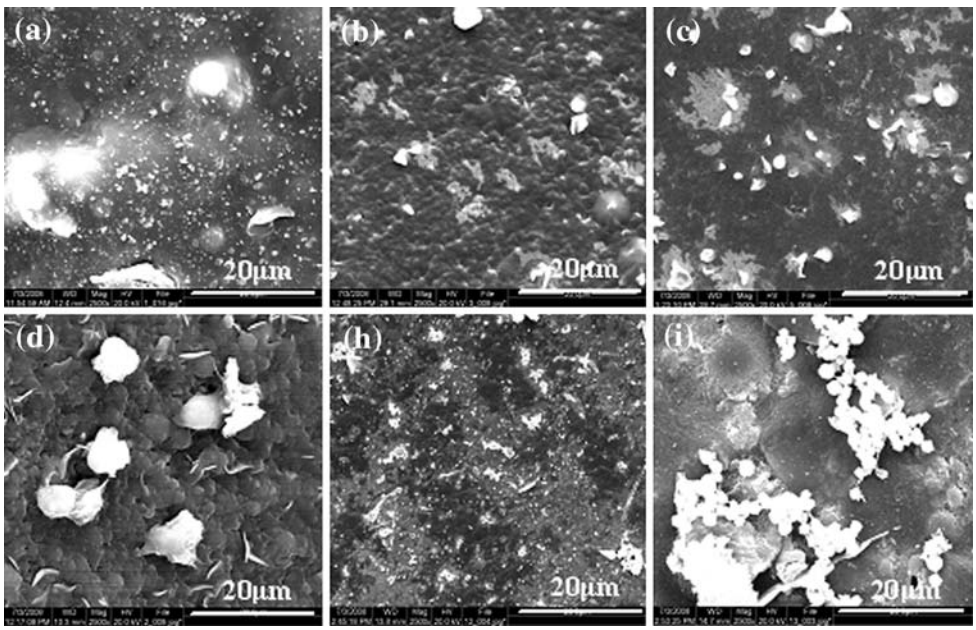

Fig. 7 SEM morphologies of adhered blood platelets on the surface of the prepared THTPBA/PEG PU samples after 1 h incubation in PRP. Herein, **a**–**d** represent samples with different feed ratios of THTPBA to PEG: **a** pure PEG, **b** 3:7, **c** 7:3, and **d** pure THTPBA; **h**, **i** represent samples containing PEG1000 and PEG4000, respectively

developed characteristic pseudopodia and large clumps of thrombi, which are typical morphologies of the activated states, suggesting poor blood compatibility [32]. In contrast, onto samples b and c with different incorporation proportion of the two components, platelet adhesion and aggregation are remarkably reduced with less extension of pseudopodia and deformation. The platelets adhered onto samples b and c are generally singular with a round shape, typical of inactivated states [33]. A smooth surface of biomaterials is generally believed to reduce or inhibit platelet activation and aggregation after the combination of THTPBA with PEG, consequently leading to the formation of less blood clot (thrombus) [32]. Another possible explanation is that the incorporation of THTPBA decreases the crystallization of PEG chain, improving anticlotting function [34]. It should note that with increasing the proportion of THTPBA, platelet loss of round shape becomes somewhat severe and extension of pseudopodia and deformation are relatively obvious. The MW of PEG has significant influence on platelet adhesion. On the surface of the THTPBA/PEG1000 and THTPBA/PEG10000 PU scaffolds, although the number of adhered platelets is increased with the MW of PEG, the platelets are generally singular and isolated with a rounded shape, which is typical of inactivated states. In contrast, for the THTPBA/PEG4000 sample, accumulation and pseudopodium of platelets are serious, and large thrombus is formed and adhered, which may be ascribed to high crystallinity in the PEG4000 PU sample. Thus, the interaction between the material and platelets is enhanced, implying decreased anticoagulated function. These results suggest that the proper incorporation of THTPBA and selection of the PEG MW may effectively reduce or restrain platelet adhesion and activation, prevent thrombus formation, and improve the blood compatibility of the PU materials, deducing that the THTPBA/PEG PU scaffolds are likely a new type of antithrombotic materials.

Cytotoxicity studies

Generally, the determination of cell viability is an assay to evaluate the in vitro cytotoxicity of biomaterials [35]. The predictive value of in vitro cytotoxicity tests is based on the concept that toxic chemicals affect the basic functions of cells. Such functions are common to all cells, and hence the toxicity can be measured by assessing cellular damage. MTT assays are a method commonly used for this purpose. In the present study, MTT assays are performed to value the effect of polymer structures on the metabolic activity of cells. All the polymers show a feed ratio and PEG MW dependent effect on cytotoxicity of HEK cells after five different culture times. Cell viabilities in the presence of various PU samples are presented in Fig. 8.

It is clear from Fig. 8a that there is no big difference among the cytocompatibility of these PU materials with various component ratios as denoted by the cell viability in line with the sample-paired t test ($p < 0.05$). Although the as-prepared THTPBA/PEG PU samples show higher cytotoxicity than the pure PEG PU one, they still produce relatively high viabilities, which is an important feature of this work, as cytotoxicity is one of the major barriers in in vitro and/or in vivo applications [28]. It can be noticed from Fig. 8b that the PEG MW has pronounced influence on the cytotoxicity. The cell viability is increased in order of PEG1000, PEG10000, and PEG4000 during the whole incubation. Higher than 90% cell viability for PEG4000 is likely due to its relatively high crystallinity and microheterogeneity [18]. In spite of this, more than 62% cell survival is still observed for the PEG1000 PU sample, indicating their low cytotoxicity. Based on the description, the THTPBA/PEG10000-based PU scaffold materials developed in this work show relatively low cytotoxicity by modulating an appropriate ratio of THTPBA to PEG (3:7), which offers us a potential option in development of biomaterials.

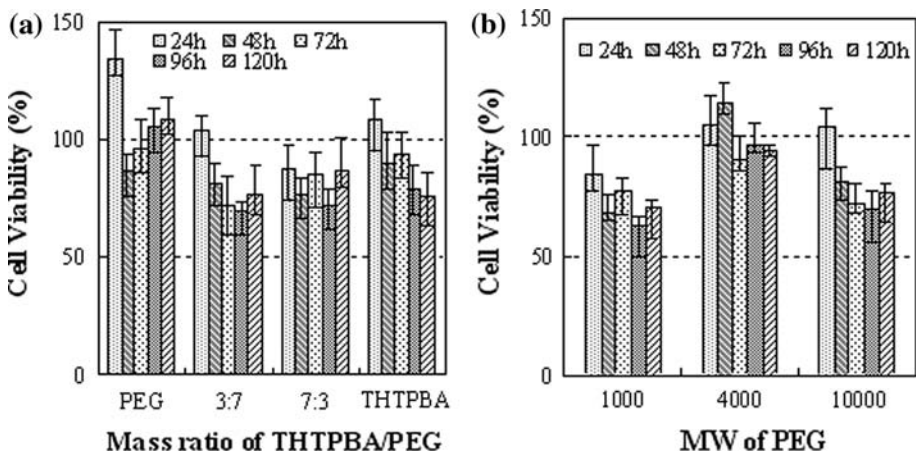

Fig. 8 Effect of **a** mass ratio of THTPBA to PEG and **b** MW of PEG on the cytotoxicity of THTPBA/PEG PU scaffolds measured by MTT assay after 24–120 h incubation with HEK cells. Each point represents the mean ± SD of five experiments

Conclusion

In summary, highly branched or crosslinked PU scaffolds have successfully been prepared on the basis of the tetra-hydroxyl-terminated THTPBA and PEG as soft segments, and HDI as a hard one. All assessments testify that hydrolytic degradation, blood compatibility, cytotoxicity and mechanical properties of the PU materials are correlated with the component ratios of THTPBA to PEG, and MW of PEG. FTIR and SEM findings indicate that the degradation of the urethane or ester linkage takes place. The mass loss is gradually enhanced with increasing the ratios and MW of PEG. Hemolysis ratio is decreased with increasing the hydrophilic component and MW of PEG. Three kinds of in vitro clotting assays proclaim that an optimized combination of the two soft segments can suppress the activation of coagulation factors and prolong the coagulation time. This combination simultaneously generates a smooth surface viewed by SEM, which remarkably reduces or inhibits platelet activation, adhesion, and aggregation, improving anticlotting properties. The dynamic coagulation assay manifests that the specimen with THTPBA to PEG ratio 3:7 appears to possess the highest absorbance and a smoother variation of optical densities, and the dissociative red cells are slightly decreased, meaning a longer clotting time or a good anti-coagulation character. MTT tests testify that the PUs show a feed ratio and MW of PEG dependent on cytotoxicity of HEK cells. The THTPBA/PEG PU samples with high MW of PEG produce over 62% cell viabilities, indicating increased proliferation and low cytotoxicity. The mechanical properties of these exploited PU scaffolds may be tailored by altering the feed ratio and molecular chain flexibility for a given application to provide desired tensile strength and modulus. Overall, the as-prepared PU materials in this work exhibit high hydrophilicity, definite biodegradation, good biocompatibility, low toxicity, and high mechanical strength. Our experience to date displays that the THTPBA/PEG PUs are an important new class of biocompatible materials and can be employed as potential candidates for blood-contacting applications.

Acknowledgements Financial support from the National Natural Science Foundation of China (Grant 10675078) is gratefully acknowledged. Thanks are due to Dr. Ling Li (Clinical Laboratory, Shaanxi Provincial People's Hospital) for her assistance in studies on hemocompatibility and coagulation time, and the authors are also grateful to Prof. Chen Huang (College of Medicine, Xi'an Jiaotong University) for her help in cytotoxicity studies.

References

1. Thomas V, Kumari TV, Jayabalan M (2001) Biomacromolecules 2(2):588
2. Stevenson JS, Kusy RP (1995) J Mater Sci Mater Med 6:377
3. Nair LS, Laurencin CT (2007) Prog Polym Sci 32:762
4. Rockwood DN, Woodhouse KA, Fromstein JD, Chase DB, Rabolt J (2007) J Biomater Sci Polym Ed 618:743
5. Grad S, Kupcsik L, Gorna K, Gogolewski S, Alini M (2003) Biomaterials 24:5163
6. Grad S, Kupcsik L, Gorna K, Gogolewski S, Alini M (2002) Eur Cell Mater 4:51
7. Guan J, Fujimoto KL, Sacks MS, Wagner WR (2005) Biomaterials 26:3961
8. Yang JM, Lin HT (2001) J Membr Sci 187:159
9. Mao S, Shuai X, Unger F, Wittmar M, Xie X, Kissel T (2005) Biomaterials 26:6343
10. Peracchia MT, Gref R, Minamitake Y, Domb A, Lotan N, Langer R (1997) J Control Release 46:223
11. Guo K, Chu CC (2007) Biomaterials 28(22):3284
12. Luo YL, Nan YF, Xu F, Chen YS, Zhao P (2009) J Biomater Sci Polymer Ed (in press)
13. Kainthan RK, Gnanamani M, Ganguli M, Ghosh T, Brooks DE, Maiti S, Kizhakkedathu JN (2006) Biomaterials 27:5377
14. Amarnath LP, Srinivas A, Ramamurthi A (2006) Biomaterials 27:1416
15. Yamanouchi D, Wu J, Lazar AN, Craig KK, Chu CC, Liu B (2008) Biomaterials 29:3269
16. Ghosh S (2004) Biomacromolecules 5:1602
17. Kolhe P, Kannan RM (2003) Biomacromolecules 4:173
18. Sun G, Zhang XZ, Chu CC (2008) J Mater Sci Mater Med 19:2865
19. Ray AR, Dey RK (2003) Biomaterials 24:2985
20. Liu JX, Yang DZ, Shi F, Cai YJ (2003) Thin Solid Films 429:225
21. Du MH, Li JS, Wei Y, Xie XY, He CS, Fan CR, Zhong YP (2003) J Biomed Eng 20:273
22. Kim J, Conway A, Chauhan A (2008) Biomaterials 29:2259
23. Zhao CX, Zhang WD (2008) Eur Polym J 44:1988
24. Jones DS, Bonner MC, Gorman SP, Akay M, Keane PF (1997) J Mater Sci Mater Med 8:713
25. Luo YL, Wang SH, Li ZQ (2008) J Mater Sci 43:174. doi: 10.1007/s10853-007-2125-5
26. Autian J (1975) In: Kronenthal RL, Oser Z, Martin E (eds) Polymer science and technology, vol 8: polymers in medicine and surgery. Plenum Press, New York
27. Guo HX, Liang CH, Mu Q (2001) Chin J Nonferrous Met 11:272
28. Liu CL, Yang DZ, Lin GQ, Qi M (2005) Mater Lett 59:3813
29. Li C, Hu GD, He YH (2003) Chin J Process Eng 3:1
30. Guo H, Jiang T, Jiang DB (2005) Chongqing Med 34:580
31. Nie FQ, Xu ZK, Huang XJ, Peng Y, Wu J (2003) Langmuir 19:9889
32. Cho HH, Han DW, Matsumura K, Tsutsumi S, Hyon SH (2008) Biomaterials 29:884
33. Pan CJ, Tang JJ, Weng YJ, Wang J, Huang N (2006) J Control Release 116:42
34. Wang DA, Ji J, Gao CY, Yu GH, Feng LX (2001) Biomaterials 22:1549
35. Draye JP, Delaey B, Voorde AV, Bulcke AVD, Reu BD, Schacht E (1998) Biomaterials 19:1677